A petro-chemical study of ancient mortars from the archaeological site of Kyme (Turkey)

Domenico Miriello[1,*], Fabrizio Antonelli[2], Carmine Apollaro[1], Andrea Bloise[1], Nicolò Bruno[3], Manuela Catalano[1], Stefano Columbu[4], Gino M. Crisci[1], Raffaella De Luca[1], Marco Lezzerini[6,7], Stefania Mancuso[5] and Antonio La Marca[5]

[1] Dipartmento di Biologia, Ecologia e Scienze della Terra (DIBEST), Università della Calabria, 87036 Arcavacata di Rende (CS), Italy
[2] Laboratorio di Analisi dei Materiali Antichi (L.A.M.A.), Università Iuav di Venezia, San Polo 2468, 30125 Venezia, Italy
[3] Soprintendenza del Mare di Palermo, via Lungarini 9, 90133 Palermo, Italy
[4] Dipartimento di Scienze Chimiche e Geologiche, Università di Cagliari, Via Trentino 51, 09127 Cagliari, Italy
[5] Dipartimento di Studi Umanistici, Università della Calabria, 87036 Arcavacata di Rende (CS), Italy
[6] Dipartimento di Scienze della Terra, Università di Pisa, Via S. Maria 53, 56126 Pisa, Italy
[7] Laboratorio di Spettroscopia Laser e Applicata, ICCOM-CNR, Area della Ricerca di Pisa, Via G. Moruzzi 1, 56124 Pisa, Italy
[*] Corresponding author: *miriello@unical.it*

Abstract

Fourteen samples of ancient mortars (joint mortars and plasters) from the archaeological site of Kyme (Turkey) were studied by optical microscopy (OM), X-ray fluorescence (XRF), X-ray powder diffraction (XRPD), scanning electron microscopy (SEM-EDS) and micro-Raman spectroscopy to obtain information about their composition.The study allowed us to identify a new type of plaster inside the archaeological site of Kyme, not detected by previous studies of this site, in which vegetable fibers were intentionally added to the mixture. The combination of a petrographic analysis on thin sections by polarized light microscopy with a chemical analysis, has allowed us to highlight similarities and differences between the mortars and to get information about the evolution of constructive techniques in the archaeological area.

Key words: Anatolia; lime lump; binder; cocciopesto; moganite; archaeometry; vegetable fibers.

Introduction

This work is the continuation of an archaeometric study, started in 2009, which has subsequently produced a first publication on the mortars of the archaeological area of Kyme (Miriello et al., 2011a). The ancient eolian city, located six kilometers south of the modern Aliağa (Figure 1), is subject of investigation and research by the Italian Mission of the University of Calabria from 2007.

The ancient city of Kyme is mentioned, by ancient historicians, like the major city of the Aeolia and was founded in the middle of the 11th century BC by populations coming from the North of Greece. In 8th century BC, its inhabitants practiced seaborne trade, and agriculture was at the basis of its economy (Mele, 1979; Lagona, 1993; 1999; Esposito et al., 2003; Lagona, 2004; La Marca, 2006; Scatozza Höricht, 2007). It was the mother country of several other cities, such as Side and probably Cuma, in the South of Italy (Ragone, 2010).

In the Hellenistic age, the city was equipped by some important monuments and building, such as the theatre (Mancuso, 2012), walls (La Marca, 2006; 2007; 2013), residential blocks on the southern hill (Frasca, 2007), as well as the enlargement of the quay (Esposito et al., 2003).

During the Imperial age, the earthquakes of AD 17 and 94 caused serious damage to the city, but Kyme managed to maintain a prestigious position, as pointed out by literary sources, some inscriptions and monuments come to light during the excavations (Honle, 1967; Manganaro, 2004).

In late Roman age and in early Byzantine age, Kyme occupied a wide area with different destinations use. In the 12th and 13th centuries, life was centred around the port and the castle built in defence of this, but recent excavations have highlighted other interesting buildings (Patitucci, 2001; Parapetti, 2004; La Marca, 2012; 2015a; 2015b). However, despite the archaeological importance of Kyme, there are still few archaeometric studies on this city (Ciminale, 2003; Miriello et al., 2011a).

The study focuses on 14 new samples of mortar sampled from different buildings of the site. The mortars are very complex artificial stone materials, which can provide important information on the construction phases of ancient buildings (Antonelli et al., 2003; Crisci et al., 2004; Riccardi et al., 2007; Carò et al., 2008; Miriello et al., 2010a; 2011b; Antonelli et al., 2012; Miriello et al., 2013a), on ancient production techniques (Franzini et al., 1999; 2000a; 2000b; Moropoulou et al., 2000; Lezzerini et al., 2005; Goldsworthy and Min, 2009; Belfiore et al., 2010; Miriello et al., 2010b; Lezzerini et al., 2014) on the provenance of raw materials (Barba et al., 2009; Barca et al., 2013; Miriello et al., 2015a; Belfiore et al., 2015; Fichera et al., 2015), but also on their deterioration phenomena (Miriello and Crisci, 2006). In this context, the petrographic study of mortars on thin section, supported by chemical, mineralogical and statistics analysis, can help the archaeologists to rebut or confirm their historical hypotheses (De Luca et al., 2013).

The aim of this work is to continue the recognition of the different types of mortars in the archaeological site of Kyme, which began in 2009, and to obtain information about their chemical, mineralogical and petrographic composition.

Materials and Methods

Two different types of mortars are studied in this work: "joint mortars" and "plasters". The joint mortars are a generic mixtures of lime, aggregates and water used to denote joining material between building stones, while the word plaster refers to a mixture of lime, aggregates and water, used to finish the surface of a wall.

Eight plasters and six joint mortars were sampled from the archaeological area of Kyme
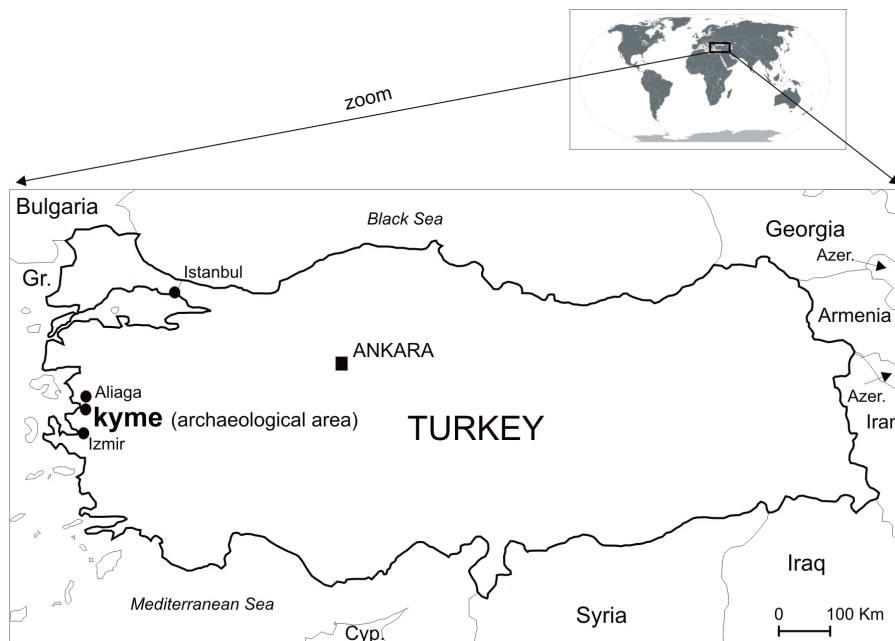
Figure 1. Location of the archaeological site of Kyme (by Miriello et al. 2011a modified).

(Table 1 and Figure 2). The plasters KM11, KM12 and KM13 come from the two churches located inside the Agorà (Figure 2a) belonging to the 5th - 7th century AD. The plasters KM33, KM34, KM35 and KM38 and the joint mortar KM37 were sampled in different areas of the Theatre (Figure 2b) and have uncertain dating. In particular KM33 and KM34 were sampled in stratigraphic continuity from the same structure. The joint mortars KM20, KM21, KM23, KM25 and KM26 come from some buildings on the seashore (Figures 2c and 2d) which dated back to the 2nd - 4th century AD, while the remaining plaster KM32 was sampled in the area of the Stoa (Figure 2e) and probably belong to the last phase of the city's history.

The petrographic, mineralogical and chemical characterization of the samples was carried out through different analytical techniques. The petrographic analysis was performed by polarized light microscopy on thin section

through a Zeiss-Axioskop 40 microscope. The sorting of the aggregate was defined by qualitative visual estimation charts, using "Textural comparators for degree of sorting in 2-D" (Jerram, 2001; Boggs, 2010). The semi-quantitative estimate of the percentages of binder, aggregate and macroporosity (d > 1/16 mm), as volume fraction, was also obtained by comparing the thin sections observed by optical microscopy with visual charts to support the estimation of modal proportions of the minerals present in the rocks (Ricci Lucchi, 1980; Myron Best, 2003).

The semi-quantitative mineralogical composition of the samples was studied by X-ray Powder Diffraction (XRPD), using a Bruker D8 Advance X-ray powder diffractometer, with Cu-Ka radiation, operating at 40 kV and 40 mA. Scans were collected in the range 3°-60° 2θ, using a step size of 0.02° 2θ and a step counting time of 0.4 s. The EVA software program

Table 1. List of samples taken from different areas of the archaeological site of Kyme with typology, location and historical period.

Sample	Typology	Location	Probable Historical Period
KM11	Plaster	Agorà, Church 1 - abside	5th - 7th century AD
KM12	Plaster	Agorà, Church 2 - floor	5th - 7th century AD
KM13	Plaster	Agorà, Church 1 - north wall	5th - 7th century AD
KM20	Joint mortar	Buildings on the seashore	2nd - 4th century AD ?
KM21	Joint mortar	Buildings on the seashore	2nd - 4th century AD ?
KM23	Joint mortar	Buildings on the seashore	2nd - 4th century AD ?
KM25	Joint mortar	Buildings on the seashore	2nd - 4th century AD ?
KM26	Joint mortar	Buildings on the seashore	2nd - 4th century AD ?
KM32	Plaster	Area of the Stoa - floor	Last phase of the city ?
KM33	Plaster	Theater - eastern hydraulic structure	After 3th century AD ?
KM34	Plaster	Theater - eastern hydraulic structure	After 3th century AD ?
KM35	Plaster	Theater - central hydraulic structure	After 3th century AD ?
KM37	Joint mortar	Theater - western hydraulic structure, horizontal surface	After 3th century AD ?
KM38	Plaster	Theater - wall of the Pulpitum	After 3th century AD ?

(DIFFRACplus EVA) was used, by comparing experimental peaks with PDF2 reference patterns in order to identify the mineralogical phases in each X-ray powder spectrum.

The chemical composition of the samples was detected by X-ray fluorescence (XRF) using a Bruker S8 Tiger WD X-ray fluorescence spectrometer, with a rhodium tube (intensity 4 kW and XRF beam of 34 mm) on powder pellets made up of 6 g of specimen placed over boric acid (maximum working pressure 25 bar). The analysis allowed us to determine the chemical composition of major (SiO_2, TiO_2, Al_2O_3, Fe_2O_3, MnO, MgO, CaO, Na_2O, K_2O, P_2O_5) and trace elements (Ni, Cr, V, La, Ce, Co, Nb, Y, Sr, Zr, Cu, Zn, Rb) present in the samples. XRF data were also processed by the Aitchison's model regarding compositional data (Aitchison, 1982; 1983,; 1986), using centred-log-ratio transformations (clr) and they were, subsequently, subjected to multivariate cluster analysis using the software IBM SPSS Statistics 22. XRF and Cluster analysis was performed on all samples, except for KM11 and KM13 where the sample was too small to perform an XRF analysis.

To study the micro-chemical composition of the binder, energy-dispersive X-ray spectroscopic
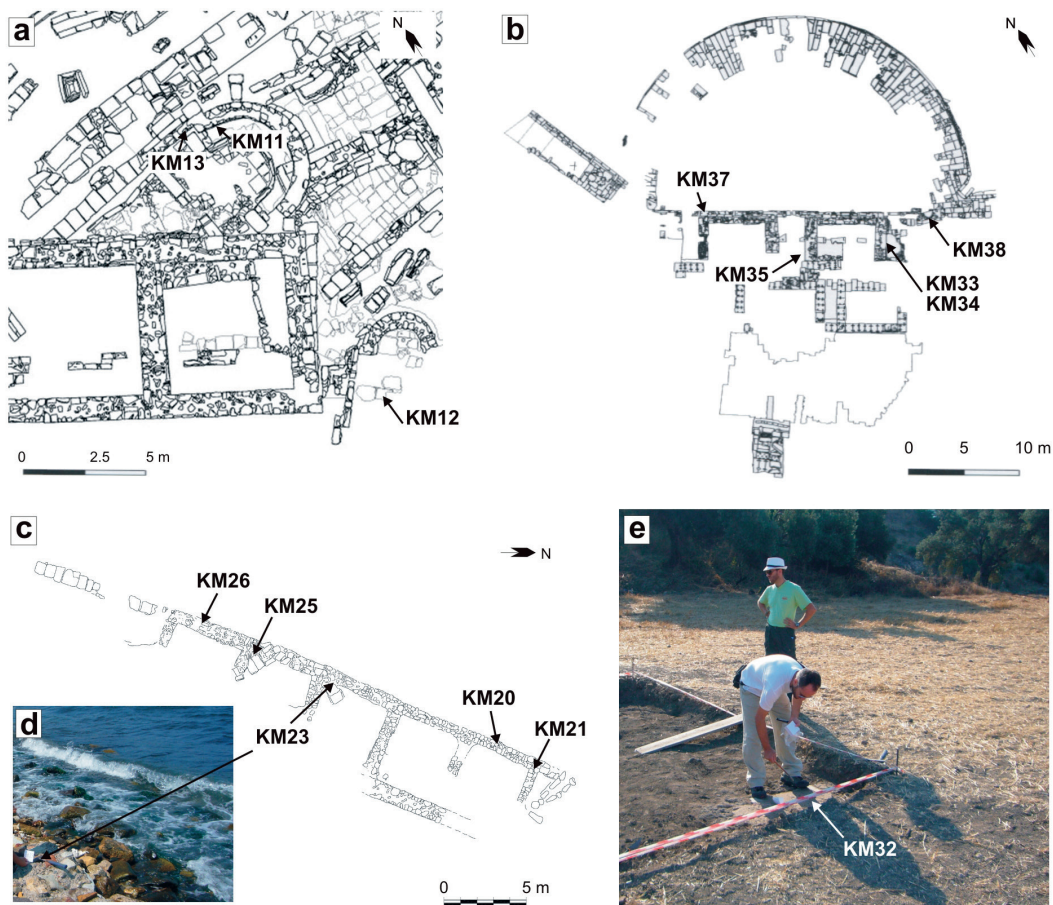
Figure 2. Sampling of the mortars with the location of the samples. a) Sketch map of the Agora with location of the plaster samples in Church 1 and Church 2; b) Sketch map of the Theatre with location of joint mortar and plaster samples; c) Sketch map of the building on the seashore with location of the joint mortar samples; d) Sampling of joint mortar KM23; e) Sampling of plaster KM32 in the area of the Stoa.

microanalysis (SEM-EDS), was performed on thin sections, using a scanning electron microscopy FEI Quanta 200 instrument, equipped with an EDAX Si (Li detector).

Raman spectroscopy was also carried out through a Thermo Fisher DXR Raman microscope, equipped with OMNICxi Raman Imaging software 1.0, to study fibrous microcrystalline quartz inside sample KM25.

The 532 nm line was used at an incident power output of 8 mW.

Results and Discussion

Macroscopic features of the samples

From the macroscopic point of view, the joint mortars (samples KM20, KM21, KM23, KM25, KM26 and KM37) have a light gray
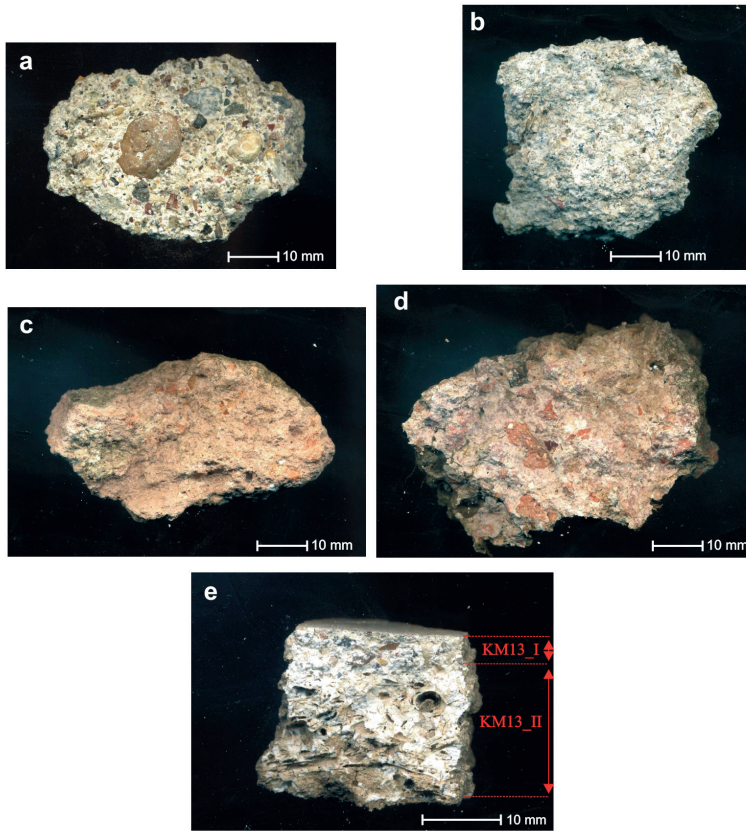
Figure 3. Macroscopic image of the samples a) KM23; b) KM25; c) KM32; d) KM38; e) KM13.

color, but different features in the size of the aggregates. Samples KM23 (Figure 3a) and KM26 is "granule" according to the Wentworth scale (1922). Samples KM20 and KM25 (Figure 3b) are "coarse sand", while samples KM21 and KM37 are "sand" (Wentworth, 1922).

Macroscopically, the plasters can be divided into two groups. The first group is made by plasters that mainly contain ceramic fragments in the aggregate ("*cocciopesto*"). It includes samples KM32, KM33, KM34 and KM38 that show a pink color. In the samples KM34 and KM38 (Figure 3d) the size of the aggregate is "pebble" (Wentworth, 1922), while the samples KM32 (Figure 3c) and KM33 are "very coarse
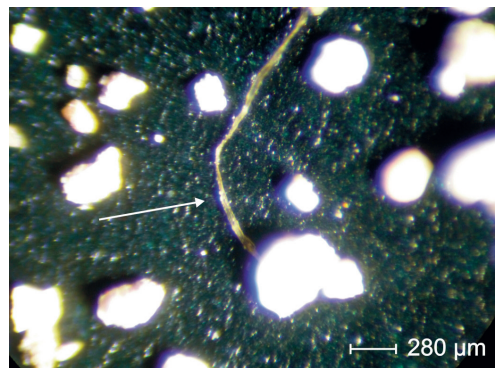

Figure 4 Microphotograph under reflected light of vegetable fiber after the extraction from sample KM13_II.

Table 2. Chemical composition of major elements of the samples by XRF analysis.

wt%	SiO_2	TiO_2	Al_2O_3	Fe_2O_3	MnO	MgO	CaO	Na_2O	K_2O	P_2O_5	L.O.I.	Sum
KM12	30.60	0.14	4.82	0.83	0.02	0.68	33.94	0.61	2.12	0.24	26.00	100.00
KM20	43.12	0.27	6.17	2.43	0.05	3.81	19.38	3.00	2.18	0.24	19.36	100.00
KM21	35.73	0.71	7.55	2.39	0.11	3.76	17.47	9.18	6.02	0.38	16.71	100.00
KM23	38.67	0.31	5.68	2.57	0.05	4.72	19.65	4.07	2.12	0.18	21.97	100.00
KM25	40.80	0.41	7.18	2.21	0.07	1.68	19.34	5.88	3.49	0.53	18.40	100.00
KM26	45.75	0.36	6.73	2.74	0.06	3.14	15.08	5.17	3.42	0.16	17.40	100.00
KM32	44.00	0.59	11.11	4.67	0.10	2.33	17.18	0.65	2.36	0.24	16.76	100.00
KM33	34.43	0.29	5.84	2.31	0.05	1.45	28.24	0.55	1.82	0.29	24.74	100.00
KM34	42.74	0.46	9.20	4.10	0.09	2.45	20.46	0.60	2.15	0.34	17.41	100.00
KM35	36.89	0.21	5.15	1.78	0.05	1.61	27.69	0.43	1.25	0.19	24.75	100.00
KM37	39.58	0.24	5.95	1.99	0.05	1.40	25.82	0.36	1.32	0.25	23.04	100.00
KM38	43.72	0.51	11.37	4.35	0.10	2.06	18.64	0.27	2.24	0.22	16.51	100.00

Table 3. Chemical composition of trace elements of the samples by XRF analysis.

| ppm	Ni	Cr	V	La	Ce	Co	Nb	Y	Sr	Zr	Cu	Zn	Rb
KM12	18	11	14	n.d.	24	n.d	11	10	349	70	11	18	92
KM20	52	108	41	n.d.	44	2	12	14	453	85	18	68	83
KM21	49	126	75	n.d.	68	9	n.d	16	544	n.d	36	37	n.d.
KM23	50	95	54	11	47	8	12	13	693	92	39	46	71
KM25	42	79	44	24	56	7	19	19	473	167	14	30	119
KM26	52	88	66	7	37	6	13	15	431	108	16	66	98
KM32	80	178	80	21	64	14	19	24	456	166	13	50	106
KM33	44	83	38	8	51	6	12	14	524	98	16	48	71
KM34	73	128	71	31	65	12	15	21	442	138	25	154	98
KM35	30	62	33	n.d.	50	2	11	13	382	79	18	92	50
KM37	37	79	37	n.d.	51	2	12	15	391	82	10	137	59
KM38	74	103	65	22	70	11	17	24	395	166	20	64	97

n.d. = not determined.
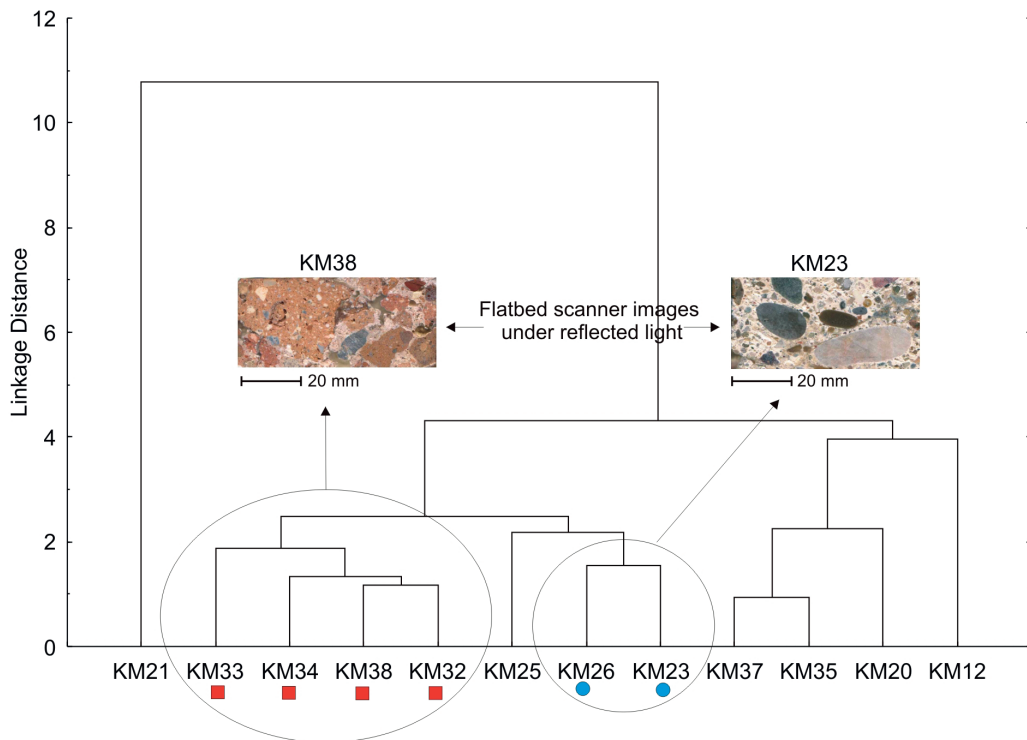
Figure 5. Cluster analysis performed on the samples considering all major and trace elements (except for samples KM11 and KM13 where the amount of the sample was too little to perform XRF analysis). Chemical data were processed using centred-log-ratio (clr) transformations (Aitchison, 1982; 1983; 1986). With the square symbol are shown mortars containing manly ceramic fragments in the aggregate; with the circle symbol are shown mortars without ceramic fragments that have the mean aggregate size greater than the other samples.

sand". Other plasters (KM11, KM12, KM13 and KM35) have a light gray color (Figure 3e). Samples KM11 and KM13 show two different layers; we indicate with "I" the outer layer (KM11_I and KM13_I) and with "II" the inner layer (KM11_II and KM13_II). The size of the aggregate of samples KM11_I, KM12 and KM13_I corresponds to "very coarse sand", "medium sand" for samples KM11_II and KM13_II, and coarse sand for sample KM35. In the plaster samples is interesting the presence of the vegetable fibers (Figure 4), which were found only in the inner layer of samples KM11 (KM11_II) and KM13 (KM13_II).

Compositional features

The compositional study of archaeological mortars must be carried out with great attention, especially when the mortars are subjected to extreme conditions of burial in archaeological sites very close to the sea, where weathering processes can significantly change the initial chemical and mineralogical composition of the samples. This is the case of samples KM20, KM21, KM23, KM25 and KM26, which were sampled on the seashore (Figure 2d). Another complication is that the mortars are heterogeneous materials, thus for the recognition of different types of mortars
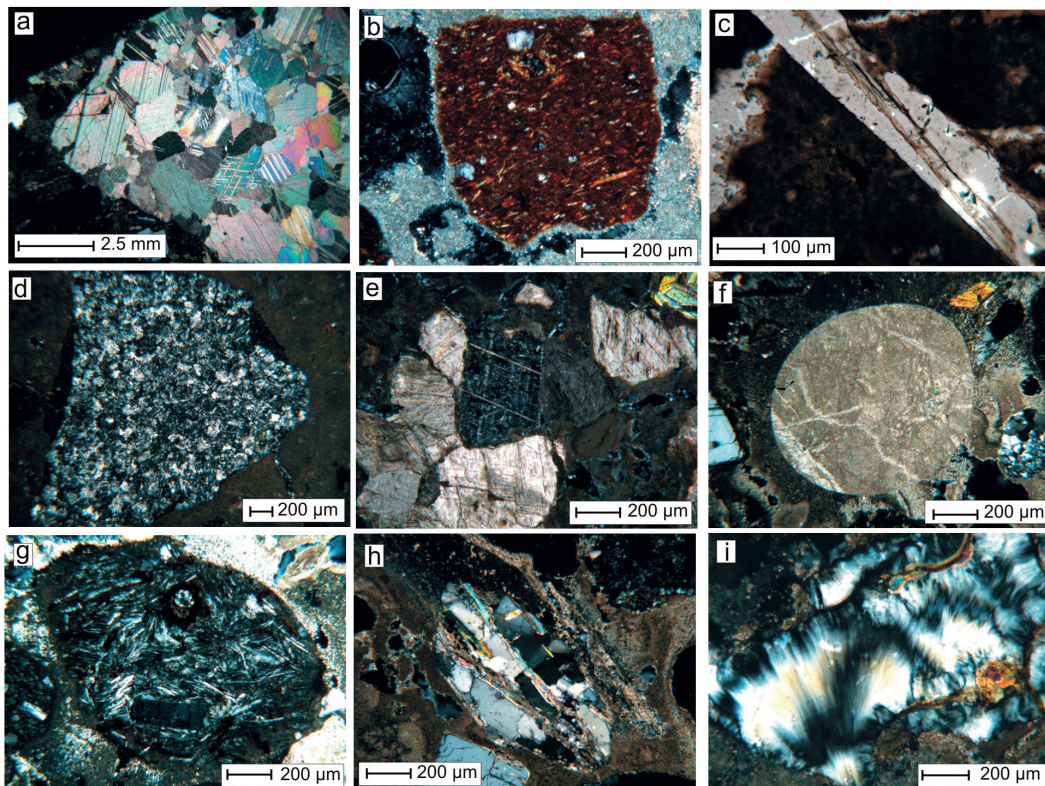
Figure 6. Microphotographs of a) Marble fragment in the sample KM21; b) Ceramic fragment (cocciopesto) in the sample KM13_I; c) Vegetable fiber in the sample KM11_II; d) Chert fragment in the sample KM11_II; e) Marble fragment in the sample KM12; f) Microcrystalline limestone in the sample KM23 ; g) Trachy-andesite in the sample KM26; h) Phyllite in the sample KM26; i) Fibrous microcrystalline quartz (chalcedony) in the sample KM25. All microphotographs were taken at crossed polars, except for "c" which is in plane polars light.

a step-by-step process is needed. Firstly, we applied the cluster analysis on all, in order to gather preliminary information on the chemical similarities between the archaeological mortars. The cluster analysis was performed considering, simultaneously, all major and trace elements (Tables 2 and 3). Results are shown in Figure 5. The dendrogram shown in Figure 5 allows to group mortars that already show macroscopic extremely different features: samples that prevalently contain ceramic fragments in the aggregate (KM32, KM33, KM34, KM38)

and mortars without ceramic fragments with a greater mean aggregate size than the other samples (KM23, KM26).

Another sample that significantly differs from the others is the joint mortar KM21 (Figure 5). From the comparison of the mineralogical data (Table 5) and the thin section study (Table 4), it is possible to observe that sample KM21 is characterized by the presence of many marble fragments larger than 2 mm in size in the aggregate (Figure 6a); besides, it has a macroporosity of about 30% and a

Table 4. Petrographic features of the samples on thin section by polarizing microscope.

	Max. aggregate size (mm)	Mean aggregate size (mm)	Wentworth size	Max. macropores (d>1/16mm) size	Mean. macropores size (mm)	Mean Roundnes	Sorting	Aggregate (%)
KM11_I	1.98	1.12	Very coarse sand	1.47	0.65	SA	MS	18
KM11_II	4.48	0.80	Medium sand	4.74	0.63	SA	MS	5
KM12	3.04	1.19	Very coarse sand	10.02	1.15	SR	MS	32
KM13_I	3.15	1.26	Very coarse sand	1.67	0.42	SA	MS	25
KM13_II	3.39	0.46	Medium sand	6.63	1.28	SA	MS	2.5
KM20	5.81	1.12	Very coarse sand	9.71	0.83	SR	MS	38
KM21	8.61	0.74	Coarse sand	5.13	1.08	SA	MS	45
KM23	15.67	2.67	Granule	5.02	1.41	SR	PS	35
KM25	7.21	1.69	Very coarse sand	3.66	1.46	SR	MS	30
KM26	12.19	3.21	Granule	4.27	1.59	SR	PS	35
KM32	0.59	1.62	Very coarse sand	7.62	1.13	SA	MS	38
KM33	8.39	1.80	Very coarse sand	6.32	1.31	SR	MS	30
KM34	19.87	5.92	Pebble	7.69	1.44	SA	PS	32
KM35	2.68	0.97	Coarse sand	3.49	1.20	SR	MWS	22
KM37	5.59	0.90	Coarse sand	3.40	1.21	SR	MS	22
KM38	19.88	5.78	Pebble	4.64	1.91	SA	PS	35

SA = sub angular; SR = sub rounded (Boggs. 2010); MS = moderately sorted; MWS = moderately well sorted; PS = poorly sorted (Jerram, 2001; Boggs, 2010). Mineralogical phases: Amp = amphibole; Bt = biotite; Cal = calcite; Chl = chlorite; Ms = muscovite; Om = opaque minerals; Or = orthoclase; Pl = plagioclase; Px = pyroxene; Qzt = quartz.

Table 4. Continued…

	Binder (%)	Macroporosity% (d>1/16mm)	A/L	Mineralogical phases of the aggregate	Ceramic fragments (Cocciopesto)	Rock fragments	Other
KM11_I	74.5	7.5	0.24	Qzt, Pl, Or, Om, Bt, Ms	Yes	Trachy-andesites, microcrystalline limestones	-
KM11_II	80	15	0.06	Qzt, Pl, Cal, Om, Ms	No	Trachy-andesites, cherts	Vegetable fibers
KM12	48	20	0.67	Qzt, Pl, Cal, Px, Ms, Bt, Om	No	Trachy-andesites, marble, rhyolites, quartzites	-
KM13_I	65	10	0.38	Qzt, Pl, Or, Om, Bt, Ms	Yes	Trachy-andesites, microcrystalline limestones	-
KM13_II	77.5	20	0.03	Qzt, Pl, Cal, Om, Ms	No	Trachy-andesites, cherts	Vegetable fibers
KM20	37	25	1.03	Qzt, Cal, Pl, Or, Ms, Bt, Amp, Px, Om	No	Trachy-andesites, quartzites, phyllites	Bioclasts
KM21	25	30	1.80	Qzt, Cal, Pl, Ms, Bt, Px, Om	No	Trachy-andesites, rhyolites, marble, quartzites	-
KM23	55	10	0.64	Qzt, Pl, Cal, Or, Ms, Bt, Px, Chl, Om	No	Microcrystalline limestones, trachy-andesites, phyllites, quartzites	Bioclasts
KM25	60	10	0.50	Qzt, Pl, Or, Cal, Px, Ms, Bt, Om	No	Trachy-andesites, rhyolites, quartzites	-
KM26	53	12	0.66	Qzt, Pl, Cal, Or, Ms, Bt, Px, Chl, Om	No	Microcrystalline limestones, trachy-andesites, phyllites, quartzites	Bioclasts
KM32	47	15	0.81	Qzt, Pl, Or, Ms, Bt, Om, Px	Yes	Trachy-andesites, microcrystalline limestones	-
KM33	52	18	0.58	Qzt, Pl, Or, Bt, Ms, Om, Px	Yes	Microcrystalline limestones, quartizites, trachy-andesites	Bioclasts
KM34	46	22	0.70	Qzt, Pl, Or, Cal, Ms, Bt, Om, Px	Yes	Microcrystalline limestones, quartizites, trachy-andesites	Bioclasts
KM35	63	15	0.35	Qzt, Pl, Or, Cal, Px, Om Bt, Ms	No	Quartzites, microcrystalline limestones, trachy-andesites	Bioclasts
KM37	68	10	0.32	Qzt, Pl, Or, Cal, Bt, Ms, Px, Om	No	Quartzites, microcrystalline limestones, trachy-andesites	Bioclasts
KM38	53	12	0.66	Qzt, Pl, Or, Om, Ms, Bt	Yes	Trachy-andesites (traces)	-

SA = sub angular; SR = sub rounded (Boggs. 2010); MS = moderately sorted; MWS = moderately well sorted; PS = poorly sorted (Jerram, 2001; Boggs, 2010). Mineralogical phases: Amp = amphibole; Bt = biotite; Cal = calcite; Chl = chlorite; Ms = muscovite; Om = opaque minerals; Or = orthoclase; Pl = plagioclase; Px = pyroxene; Qzt = quartz.

Table 5. Semi-quantitative mineralogical composition of the samples in order of decreasing relative abundance. detected by XRPD analysis.

	Max ←	—	—	—	—	—	—	→ Min
KM11	Cal	Qzt	Pl	Or				
KM12	Cal	Qzt	Pl	Mnt				
KM13	Cal	Qzt						
KM20	Qzt	Cal	Pl	Dol	Hl	Mca		
KM21	Cal	Qzt	Hl	Pl	Dol	He	Chl	Mca
KM23	Qzt	Cal	Hl	Dol	Pl	Chl	Mica	
KM25	Cal	Qzt	Pl	Hl	Dol	He		
KM26	Qzt	Cal	Hl	Pl	Dol	Mca	Chl	
KM32	Cal	Qzt	Pl	Or	Mca	Dol		
KM33	Cal	Qzt	Pl	Mnt				
KM34	Qzt	Cal	Pl	Dol	Mca	Mnt		
KM35	Qzt	Cal	Pl	Or	Mca			
KM37	Cal	Qzt	Pl	Or	Mca			
KM38	Cal	Qzt	Pl	Or	Mca			

Cal = Calcite; Chl = Chlorite; Dol = Dolomite; He = Heulandite; Hl = Halite; Mca = Mica; Mnt = Montmorillonite; Or = Orthoclase; Pl = Plagioclase; Qzt = Quartz.
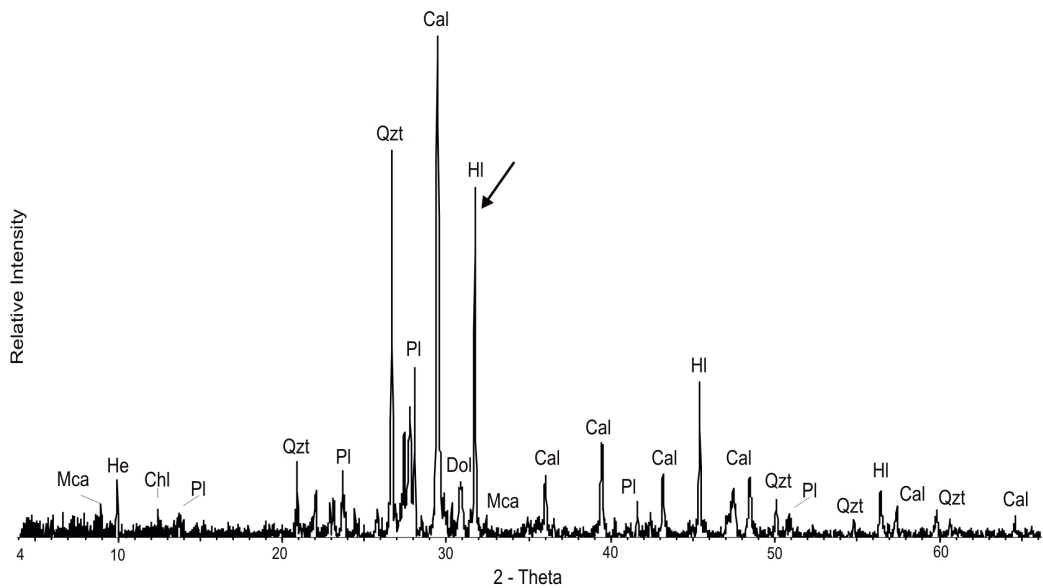

Figure 7. X-ray diffraction patterns of sample KM21 with identification of the principal mineralogical phases (Cal = Calcite; Chl = Chlorite; Dol = Dolomite; He = Heulandite; Hl = Halite; Mca = Mica; Pl = Plagioclase; Qzt = Quartz).
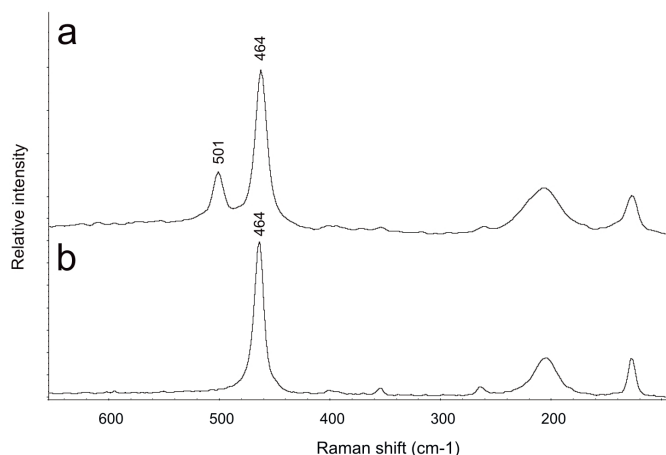
Figure 8. a) Raman spectra of fibrous microcrystalline quartz (chalcedony) in sample KM25 shown in figure 6i; b) Raman spectra of a quartz crystal belonging to the collection of the Department of Biology. Ecology and Earth Sciences (Calabria University - Italy).

high content of secondary halite (NaCl), due to the precipitation of salts by sea water (Table 5 and Figure 7). In addition to marble fragments, KM21 also contains trachy-andesite, rhyolite and quartzite rock fragments. Apparently the dendrogram (Figure 5) shows the presence of a macro-group that contains the samples KM12, KM20, KM35 and KM37, but as it will be possible to see after, significant petrographic differences there are between these samples.

In the dendrogram shown in Figure 5, the samples that are inside the same cluster have a high chemical affinity, but this is not sufficient to consider the samples belonging to the same construction phase, because they may have completely different mineralogical and petrographic features. The petrographic study of the thin sections by polarized microscope allows us to explore this issue in more detail.

Petrographic observations in thin section of samples KM11 and KM13 show that they are very similar plasters. Both samples are made of a thin top layer (KM11_I and KM13_I) with a thickness of about 5 mm, in which the aggregate contains ceramic fragments (Figure 6b), trachy-andesite and microcrystalline limestone rock fragments (Table 4). The inner layer (KM11_II; KM13_II), which is thicker, is composed mainly by vegetable fibers (Figure 4 and 6c) with traces of trachy-andesite and chert (Figure 6d) rock fragments.

Although sample KM12 should belong to the same historical period as samples KM11 and KM13 (5th - 7th century AD), it does not contain vegetable fibers in the aggregate, but it has finely crushed marble (Fgure 6e), trachy-andesite, rhyolite and quartzite rock fragments.

Samples KM23 and KM26, which are inside the same cluster assample KM25 (Figure 5), have aggregates made of very rounded rock fragments of different typologies, as microcrystalline limestones (Figure 6f), trachy-andesites (Figure 6g), phyllites (Figure 6h) and quartzites. Rare bioclasts also occur.

Contrariwise, the sample KM25 has the average size of the aggregate smaller than samples KM23 and KM26, and it does not contains limestones and bioclasts, but only trachy-andesite, rhyolite and quartzite rock

Table 6. Average values of the chemical composition of the binder in the mortars, performed by SEM-EDS microanalysis.

wt%	SiO_2	Al_2O_3	Fe_2O_3	MgO	CaO	Na_2O	K_2O	Cl	SO_3
KM11_I	4.52	1.46	n.d.	1.10	92.21	n.d.	n.d.	0.71	n.d.
KM11_II	2.96	1.35	n.d.	0.97	94.13	n.d.	n.d.	0.59	n.d.
KM12	7.88	3.58	n.d.	0.70	86.10	n.d.	n.d.	0.91	0.82
KM13_I	3.99	1.36	n.d.	1.17	92.63	n.d.	n.d.	0.85	n.d.
KM13_II	2.33	1.11	n.d.	0.98	94.80	n.d.	n.d.	0.79	n.d.
KM20	23.99	5.41	0.46	2.09	61.84	1.44	0.48	1.74	2.57
KM21	24.70	5.86	0.66	2.31	60.52	1.76	0.81	2.04	1.34
KM23	27.96	5.00	0.90	1.80	58.28	2.13	1.37	1.60	0.96
KM25	7.60	1.67	n.d.	0.89	86.35	0.51	n.d.	1.09	1.89
KM26	28.20	4.76	n.d.	1.84	60.17	1.14	1.38	1.56	0.95
KM32	21.49	6.65	1.03	1.36	68.68	n.d.	n.d.	n.d.	0.78
KM33	34.57	7.59	1.02	1.44	53.61	n.d.	0.92	0.85	n.d.
KM34	32.08	8.78	0.79	2.05	52.92	0.83	0.78	0.71	1.06
KM35	37.01	7.62	n.d.	1.76	50.02	0.78	0.82	0.71	1.28
KM37	38.76	7.67	n.d.	1.71	48.58	0.64	0.64	0.72	1.29
KM38	27.47	8.27	0.77	3.05	58.69	n.d.	1.00	n.d.	0.75

n.d. = not determined.

fragments. Furthermore, in the sample KM25 it is possible to observe the presence of chalcedony (Figure 6i), forming a spatial arrangement of 50-100 nm sized α-quartz crystallites (Rios et al., 2001; Schmidt et al., 2013). A characterization of fibrous microcrystalline minerals shown in Figure 6i was perfomend by μ-Raman spectroscopy, a technique pivotal in Cultural Heritage for studying stone materials (Baita et al., 2014); as shown in the Raman spectra of Figure 8, the typical 464 and 501 cm^{-1} marker bands are related to symmetric stretching-bending vibrations of α quartz and moganite respectively (Flörke et al., 1976; 1984; Kathleen and Russell, 1994; Götze et al., 1998; Schmidt et al., 2012; 2013). The presence of chalcedony in the aggregate of the sample, in the future, might be useful to determine the provenance of the sand used in the preparation of the mortars.

Samples KM35 and KM37 have an aggregate made prevalently by monocrystalline fragments of quartz, plagioclase, orthoclase, opaque minerals, biotite and muscovite; quartzite, microcrystalline limestone, trachy-andesite rock fragmensts are present in smaller quantity compared to all other samples.

The sample KM20 is different from the other samples, because it contains some crystals of clinopyroxene with skeletal habit (Figure 9a) and many volcanic rock fragments with inside some crystals of amphybole with opacite rims (Figure 9).

The dendrogram in Figure 5, built on chemical base, has allowed to group all of the samples in which the aggregate is composed primarily of ceramic fragments (KM32, KM33, KM34, KM38). In actual fact, the study of these samples in thin section has shown significant differences between them.

Samples KM33 and KM34 were sampled in stratigraphic continuity. KM33 and KM34 are, respectively, the external and inner layer of the same stratigraphic sequence. The two samples have the same petrographic composition, with the presence of microcrystalline limestone, quartzite, trachy-andesite rock fragments and bioclasts (Figure 9c), but they have different average aggregate size (Figures 9e and 9f).

The sample KM32 (Figure 9d) contains in the aggregate trachy-andesite and microcrystalline limestone rock fragments, without the presence of bioclasts.

The aggregate of sample KM38 (Figure 9g) is made primarily of ceramic fragments, with traces of trachy-andesite rock fragments.

By combining the petrographic observations in thin section performed by the polarizing microscope with the cluster analysis built on chemical base, it is possible to define the limits between the groups of samples recognized by cluster analysis. Figure 10 shows the previous dendrogram, in which the gray rectangles
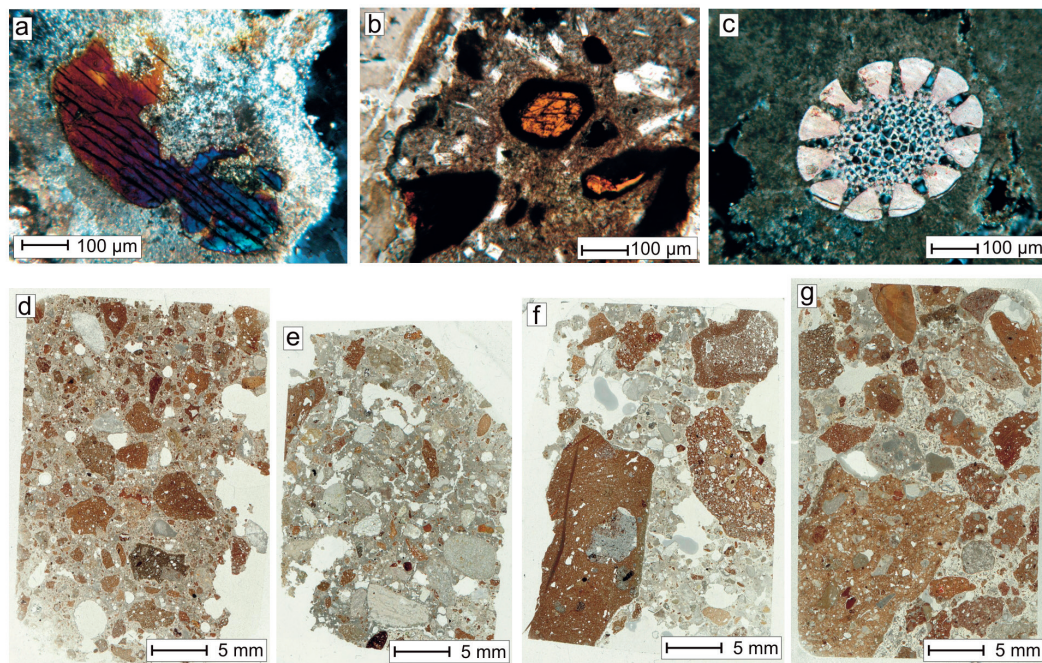

Figure 9. a) Crossed polars microphotograph of the sample KM20: clinopyroxene with skeletal habit; b) Plane-polarized light microphotograph of the sample KM20: amphybole crystals with opacite rims inside a volcanoclastic fragment; c) Crossed polars microphotograph of the sample KM34 showing an echinoid spine; d), e), f) and g) Flatbed scanner image under transmitted natural light of the samples KM32, KM33, KM34 and KM38, respectively.
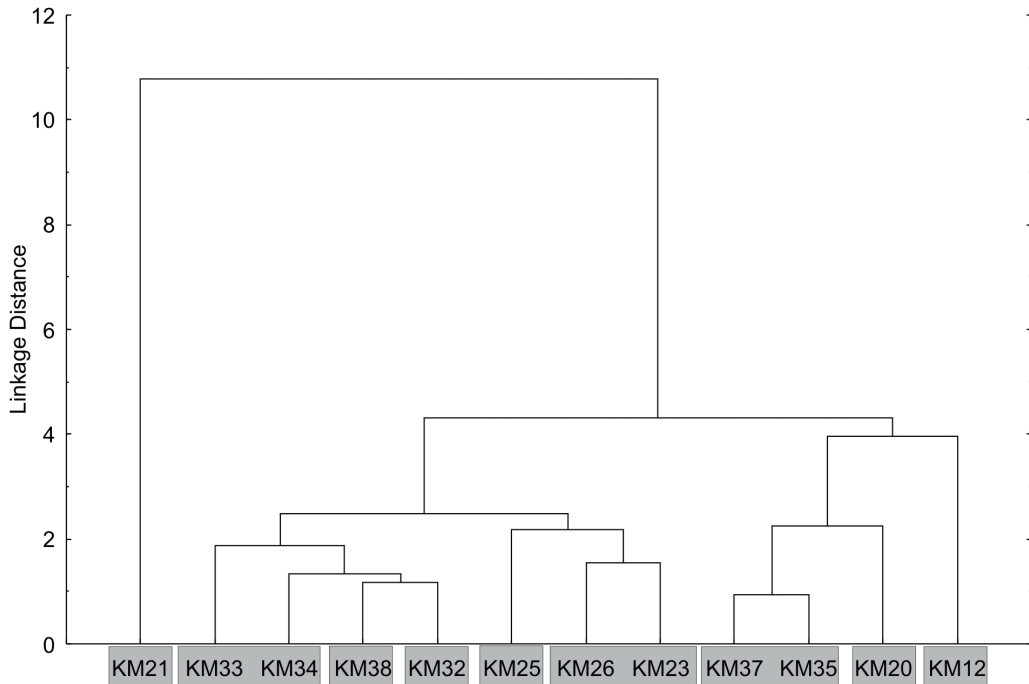
Figure 10. Cluster analysis performed on the samples considering all major and trace elements (except for the samples KM11 and KM13 where the amount of the sample was too little to perform XRF analysis). Gray rectangles enclose samples that are similar in terms of chemical and petrographic composition.

enclose samples that are similar in terms of chemical and petrographic composition. The dendrogram does not contain samples KM11 and KM13, where the sample was too small to perform an XRF analysis; but they may be theoretically enclosed within the same rectangle, because they have the same petrographic features and they are the only samples which contain vegetable fibers.

Chemical analysis of the binder

SEM-EDS microanalysis (Table 6) was performed on the binder to obtain preliminary and semi-quantitative information about the chemical composition of the lime. For all samples, microanalysis was carried out on several spots of the binder (from a minimum of 3 to a maximum of 5 spots).

Considering the average values of the chemical composition of the binder (Table 6), the percentages of CaO+MgO (wt%) decrease, while the amounts of $SiO_2+Al_2O_3+Fe_2O_3$ (wt%) increase in the samples that contain a high amount of ceramic fragments (Figure 11). The presence of this material considerably increases the hydraulicity of the mixture, involving the probable formation of calcium silicate hydrates (C-S-H phases).

However, not only the samples that contain ceramic fragments show significant hydraulic properties of the binder, but almost all the samples, except for KM11, KM12, KM13 and KM25. This is due, probably, to the influence of the volcanic rock fragments present naturally in the local raw materials used as aggregates, that most probably have pozzolanic properties.
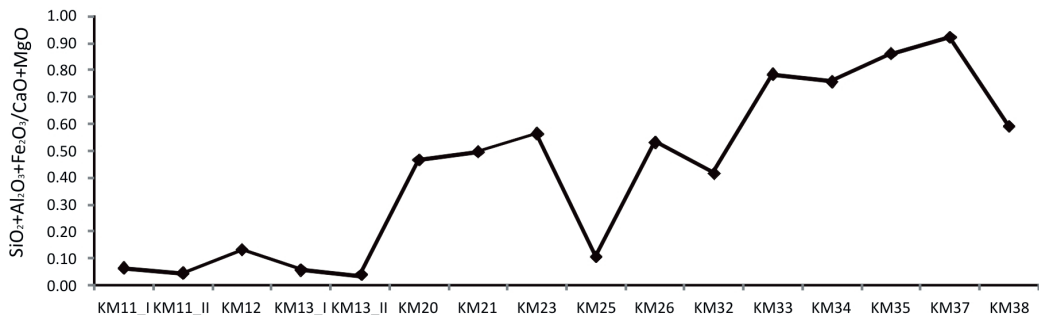
Figure 11. Chemical trend of $SiO_2+Al_2O_3+Fe_2O_3/CaO+MgO$ ratio in the binder of the mortars. (Performed by SEM-EDS microanalysis).

Future more detailed studies, focused only on volcanic materials, are needed to clarify definitively this issue.

Conclusions

The compositional study of archaeological mortars coming from the archaeological site of Kyme allows us to formulate the following considerations:

- For a correct evaluation of the similarities and differences between the ancient mortars, it is fundamental to combine the petrographic analysis on thin sections by polarized light microscopy with the chemical analysis. The statistical analysis of the data, based only on chemical variables, could give clusters of mortars petrographically inhomogeneous.

- This approach has allowed us to recognize, in Theater, three different types of mortars with different compositional features (cluster KM33 and KM34; cluster KM35 and KM37; type KM38). Probably these differences are due to the changes that have affected the stage building over time. Currently, further archaeological studies are in progress to confirm this hypothesis.

- Even though the two churches (Church 1 and Church 2) were built between the 5th and the 7th century AD, they were probably built in two different periods; in fact, samples KM11 and KM13 (from Church 1), which contain numerous vegetable fibers, are different from sample KM12 (from Church 2). This new type of plaster (with vegetable fibers) had not been recorded by previous studies carried out in this archaeological site (Miriello et al., 2011a). This technique probably appeared in Kyme between 5th and 7th century AD. The presence of vegetable fibers is not random, but they have been voluntarily added because they are uniformly present inside the samples. The use of vegetable additives in the ancient time has been well documented, especially for the plasters (Elsen, 2006; Xiao et al., 2014).Vegetable fibers have traditionally been used to improve the tensile strength (Elsen, 2006).

- The mortar KM32 (sampled from Stoa) is different from all the other samples; this would be in agreement with the hypotheses formulated by archaeologists, because this sample belongs to the last phase of the city's history.

- As regards the mortars sampled from buildings that are now on the seashore, samples KM23 and KM26 are very similar; probably they were made during the same building phase. Conversely, samples KM20, KM21 and KM25, are extremely different, as they may belong to different construction phases. However, this area of the archaeological site has hardly been studied. To explain these differences further archaeological studies are in progress.

- For the production of mortars it is possible

to hypothesize, locally, the use of aerial lime, which becomes hydraulic lime through the addition of ceramic fragments and the non-intentional presence of volcanic rock fragments.

- Comparing the composition of the cocciopesto plasters studied in this work, with the composition of the cocciopesto plasters belonging to the same historical period studied in previous work (Miriello et al., 2011a), it is possible to highlight the use of the same executive technique.

The compositional analyses of the aggregate and the binder of the mortar, combined with mixing and optimization techniques (Miriello et al., 2007; 2013b; 2015b), can be used, in the future, to produce compatible repair mortars for restoration works.

Acknowledgements

References

Aitchison J. (1982) - The statistical analysis of compositional data (with discussion). *Journal of the Royal Statistical Society, Series B (Statistical Methodology)*, 44, 139-177.

Aitchison J. (1983) - The Principal component analysis of compositional data. *Biometrika,* 70, 57-65.

Aitchison J. (1986) - The statistical analysis of compositional data. In: Monographs on Statistics and Applied Probability. Chapman & Hall Ltd, London Reprinted (2003) with Additional Material by The Blackburn Press, Caldwell, NJ.

Antonelli F., Gentili G., Renzulli A. and Amadori M.L. (2003) - Provenance of the ornamental stones used in the baroque church of S. Pietro in Valle (Fano, Central Italy) and commentary on their state of

conservation. *Journal of Cultural Heritage*, 4, 299-312.

Antonelli F., Lazzarini L. and Cancelliere S. (2012) - Minero-petrographic characterisation of the mortars and its possible application in the definition of the building phases. In: Tonghini C. (Ed.), Shayzar I. The fortification of the citadel. History of Warfare, 71, 315-323 + 4 TAV, Brill, Leiden-Boston.

Baita C., Lottici P.P., Salvioli-Mariani E., Vandenabeele P., Librenti M., Antonelli F. and Bersani D. (2014) - An integrated Raman and petrographic characterization of Italian Mediaeval artifacts in Pietra Ollare (soapstone). *Journal of Raman Spectroscopy,* 45(1), 144-122.

Barba L., Blancas J., Manzanilla L.R., Ortiz A., Barca D., Crisci G.M., Miriello D. and Pecci A. (2009) - Provenance of the limestone used in Teotihuacan (Mexico): a methodological approach. *Archaeometry*, 51, 525-545.

Barca D., Miriello D., Pecci A., Barba L., Ortiz A., Manzanilla L.R., Blancas J. and Crisci G.M. (2013) - Provenance of glass shards in archaeological lime plasters by LA-ICP-MS: implications for the ancient routes from the Gulf of Mexico to Teotihuacan in Central Mexico. *Journal of Archaeological Science*, 40, 3999-4008.

Belfiore C.M., La Russa M.F., Mazzoleni P., Pezzino A. and Viccaro M. (2010) - Technological study of "ghiara" mortars from the historical city centre of Catania (Eastern Sicily, Italy) and petro-chemical characterization of raw materials. *Environmental Earth Sciences*, 61, 995-1003.

Belfiore C.M., Fichera G.V., La Russa M.F., Pezzino A., Ruffolo S.A., Galli G. and Barca D. (2015) - A multidisciplinary approach for the archaeometric study of pozzolanic aggregate in Roman mortars: the case of Villa dei Quintili (Rome, Italy). *Archaeometry*, 57, 269-296.

Boggs S. Jr. (2010) - Petrology of sedimentary rocks, II edition; Cambridge University Press. Cambridge UK.

Carò F., Riccardi M.P. and Mazzilli Savini M.T. (2008) - Characterization of plasters and mortars as a tool in archaeological studies: the case of Lardirago Castle in Pavia, Northern Italy. *Archaeometry*, 50, 85-100.

Ciminale M. (2003) - A high-resolution magnetic mosaic at the Kyme archaeological site (Turkey). *Archaeological Prospection*, 10, 119-130.

Crisci G.M., Franzini M., Lezzerini M., Mannoni T.

and Riccardi M.P. (2004) - Ancient mortars and their binder. *Periodico di Mineralogia*, 73, 259-268.

De Luca R., Cau Ontiveros M.A., Miriello D., Pecci A., Le Pera E., Bloise A. and Crisci G.M. (2013) - Archaeometric study of mortars and plasters from the Roman City of Pollentia (Mallorca-Balearic Islands). *Periodico di Mineralogia*, 82, 3, 353-379.

Elsen J. (2006) - Microscopy of historic mortars: a review. *Cement and Concrete Research*, 36, 1416-1424.

Esposito E., Felici P.A., Gianfrotta E. and Scognamiglio E. (2003) - Il porto di Kyme. *Archeologia subacquea, Studi, ricerche e documenti*, 3, 1-37.

Fichera G.V., Belfiore C.M., La Russa M.F., Ruffolo S.A., Barca D., Frontoni R., Galli G. and Pezzino A. (2015) - Limestone Provenance in Roman Lime-Volcanic Ash Mortars from the Villa dei Quintili, Rome. *Geoarchaeology An International Journal,* 30, 79-99.

Flörke O.W., Jones J.B. and Schmincke H.U. (1976) - A new microcrystalline silica from Gran Canaria. *Zeitschrift für Kristallographie,* 143, 156-165.

Flörke O.W., Flörke U. and Giese U. (1984) - Moganite, a new microcrystalline silica-mineral. *Neues Jahrbuch Für Mineralogie-Abhandlungen,* 149, 325-336.

Franzini M., Leoni L., Lezzerini M. and Sartori F. (1999) - On the binder of some ancient mortars. *Mineralogy and Petrology*, 67, 59-69.

Franzini M., Leoni L. and Lezzerini M. (2000a) - A procedure for determining the chemical composition of binder and aggregate in ancient mortars: its application to mortars from some medieval buildings in Pisa. *Journal of Cultural Heritage*, 1, 365-373.

Franzini M., Leoni L., Lezzerini M. and Sartori F. (2000b) - The mortar of the "leaning tower" of Pisa: the product of a medieval technique for preparing high-strength mortars. *European Journal of Mineralogy,* 12, 1151-1163.

Frasca M. (2007) - Il quartiere di abitazioni della collina Sud. Prime osservazioni sulla fase romana. In: Scatozza Höricht L.A. (Ed.), Kyme e l'Eolide da Augusto a Costantino, Luciano Editore, Napoli, pp. 89-102.

Goldsworthy H. and Min Z. (2009) - Mortar studies towards the replication of Roman concrete. *Archaeometry*, 51, 932-946.

Götze J., Nasdala L., Kleeberg R. and Wenzel M. (1998) - Occurrence and distribution of "moganite"

in agate/chalcedony: a combined micro-Raman, Rietveld, and cathodoluminescence study. *Contributions to Mineralogy and Petrology,* 133, 96-105.

Honle A. (1967) - Neue Inschriften von Kyme. *Archäologischer Anzeiger*, 1, 16-62.

Jerram D.A. (2001) - Visual comparators for degree of grain-size sorting in two and three-dimensions. *Computers & Geoscience,* 27, 485-492.

Kathleen J.K. and Russell J.K. (1994) - Raman spectroscopic study of microcrystalline silica. *American Mineralogist*, 79, 269-273.

Lagona S. (1993) - Kyme Eolica: fonti, storia, topografia. *Cronache di archeologia*, 32, 19-33.

Lagona S. (1999) - Le ricerche a Kyme Eolica. *Quaderni di Topografia Antica*, 3, 1-42.

Lagona S. (2004) - Kyme alla luce delle nuove scoperte. Studi su Kyme Eolica, 2, 3-15.

La Marca A. (2006) - Il "muro di andesite" nell'area portuale di Kyme. In: Proceedings of Studi su Kyme Eolica IV, 27-48.

La Marca A. (2007) - Nuovi dati sul "muro di andesite" a Kyme d'Eolide. In: Scatozza Höricht L.A. (Ed.), Kyme e l'Eolide da Augusto a Costantino, Luciano Editore, Napoli, 71-82.

La Marca A. (2012) - Kyme 2010: Şehir ve Yayılım Alanı, Yeni topoğrafik Veriler, in Atti del Simposio Internazionale, Malatya 23-28 maggio 2011, *Arkeometri Sonuçları Toplantısı,* 2011, 27, Ankara 2012, 191-208.

La Marca A. (2013) - Kyme, hellenistik sur duvari in G. KöKdemir (ed.) Orhan Bingöl'e 67. Yas Armagani. A Festschrift for Orhan Bingöl on the occasion of his 67th birthday, Ankara, 301-315.

La Marca A. (2015a). La necropoli sud-est "Dört Yıldız" di Kyme eolica. In: Bordi G., Carlettini I., Fobelli L., Menna M.R., Pogliani P. (Ed.). L'officina dello sguardo. I Luoghi dell'arte. Immagine, memoria, materia, scritti in onore di Maria Andaloro, Roma, 633-640.

La Marca A. (2015b). Kyme 'de kutsal ala. *Journal of Archaelogy & Art*, 148, 87-98.

Lezzerini M. (2005) - The mortars of the «Fortezza delle Verrucole - S. Romano in Garfagnana (LU)». *Periodico di Mineralogia,* 74, 55-67.

Lezzerini M., Lorenzetti G., Palleschi V. and Tamponi M. (2014) - Characterization of historical mortars from the bell tower of St. Nicholas church (Pisa, Italy). *Construction and Building Materials,* 69,

203-212.

Mancuso S. (2012) - Studi su Kyme Eolica V il Teatro: attività delle campagne di scavo 2006-2011. Rubettino, Soveria Mannelli.

Manganaro G. (2004) - Nuove iscrizioni greche di Kyme. Studi su Kyme Eolica, 2, 49-58.

Mele A. (1979) - Il commercio greco arcaico. Prexis ed emporie. *Chaiers du centre J. Bèrard,* 4, 1-109.

Miriello D. and Crisci G.M. (2006) - The Image analysis and flatbed scanners. A visual procedure in order to study the macro-porosity of the archeological and historical mortars. *Journal of Cultural Heritage*, 7, 186-192.

Miriello D. and Crisci G.M. (2007) - The Mixing and provenance of raw materials in the bricks from the Svevian castle of Rocca Imperiale (North Calabria - Italy). European *Journal of Mineralogy*, 19, 137-144.

Miriello D., Barca D., Bloise A., Ciarallo A., Crisci G.M., De Rose F., Gattuso C., Gazineo F. and La Russa M.F. (2010a) - Characterisation of archaeological mortars from Pompeii (Campania, Italy) and identification of construction phases by compositional data analysis. *Journal of Archaeological Science*, 37, 2207-2223.

Miriello D., Bloise A., Crisci G.M., Barrese E. and Apollaro C. (2010b) - Effects of milling: a possible factor influencing the durability of historical mortars. *Archaeometry*, 52, 668-679.

Miriello D., Bloise A., Crisci G.M., Apollaro C. and La Marca A. (2011a) - Characterisation of archaeological mortars and plasters from Kyme (Turkey). *Journal of Archaeological Science,* 38, 794-804.

Miriello D., Barca D., Crisci G. M., Barba L., Blancas J., Ortiz A., Pecci A. and López L.L. (2011b) - Characterization and provenance of lime plasters from the Templo Mayor of Tenochtitlan (Mexico City). *Archaeometry*, 53, 1119-1141.

Miriello D., Bloise A., Crisci G.M, Cau Ontiveros M.Á., Pecci A. and Riera Rullan M. (2013a) - Compositional analyses of mortars from the late Antique site of Son Peretó (Mallorca, Balearic Islands, Spain): archaeological implications. *Archaeometry*, 55, 1101-1121.

Miriello D., Lezzerini M., Chiaravalloti F., Bloise A., Apollaro C. and Crisci G.M. (2013b) - Replicating the chemical composition of the binder for restoration of historic mortars as an optimization

problem. *Computers and Concrete,* 12, 553-563.

Miriello D., Barca D., Pecci A., De Luca R., Crisci G.M., López Luján L. and Barba L. (2015a) - Plasters from different buildings of the Sacred Precinct of Tenochtitlan (Mexico City): characterization and provenance. *Archaeometry*, 57, 100-127.

Miriello D., Bloise A., De Luca R., Apollaro C., Crisci G.M., Medaglia S., Taliano Grasso A. (2015b) - First compositional evidences on the local production of Dressel 2-4 amphorae in Calabria (Southern Italy): characterization and mixing simulations. *Applied Physics A Materials Science & Processing,* 119, 1595-1608.

Moropoulou A., Bakolas A. and Bisbikou K. (2000) - Investigation of the technology of historic mortars. *Journal of Cultural Heritage,* 1, 45-58.

Myron Best G. (2003) - Igneous and metamorphic petrology. Second Edition. Wiley Blackwell Publishing. New York.

Parapetti R. (2004) - Il castello medievale a Kyme. Studi su Kyme Eolica, 2, 59-70.

Patitucci U. (2001) - Kyme Eolica e il Castello Bizantino. *Rendiconti Pontificia Accademia* LXXII, 1999-2000, 47-112.

Ragone G. (2010) - Cuma eolica, in Cuma. Atti del XLVIII Convegno di Studi sulla Magna Grecia Taranto 2008, Taranto, 37-72.

Riccardi M.P., Lezzerini M., Carò F., Franzini M. and Messiga B. (2007) - Microtextural and microchemical studies of hydraulic ancient mortars: two analytical approaches to understand pre-industrial technology processes. *Journal of Cultural Heritage,* 8, 350-360.

Ricci Lucchi F. (1980) - Sedimentologia parte I: Materiali e tessiture dei sedimenti. Clueb, Bologna.

Rios S., Salje E.K.H. and Redfern S.A.T. (2001) Nanoquartz vs. macroquartz: a study of the a - b phase transition. *European Physical Journal B,* 20, 75-83.

Scatozza Höricht L.A. (2007) - Nuovi dati per lo studio della città di Kyme in età ellenistica romana. Le ricerche dell'Università Federico II di Napoli. In: Scatozza Höricht L.A. (Ed.), Kyme e l'Eolide da Augusto a Costantino, Luciano Editore, Napoli, 103-134.

Schmidt P., Bellot-Gurlet L., Slodczyk A. and Fröhlich F. (2012) - A hitherto unrecognised band in the Raman spectra of silica rocks: influence of hydroxylated Si–O bonds (silanole) on the Raman

moganite band in chalcedony and flint (SiO$_2$). *Physics and Chemistry of Minerals,* 39, 455-464.

Schmidt P., Bellot-Gurlet L., Lea V. and Sciau P. (2013) - Moganite detection in silica rocks using Raman and infrared spectroscopy. *European Journal of Mineralogy*, 25, 707-805.

Wentworth C.K. (1922) - A scale of grade and class terms for clastic sediments. *Journal of Geology,* 30, 377-392.

Xiao Y., Fu X., Gu H., Gao F. and Liu S. (2014) Properties, characterization, and decay of sticky rice-lime mortars from the Wugang Ming dynasty city wall (China). *Materials Characterization,* 90, 164-172.